Published in final edited form as:
Ultrasound Med Biol. 2010 November ; 36(11): 1907–1918. doi:10.1016/j.ultrasmedbio.2010.05.014.

ANALYSIS OF *IN VITRO* TRANSFECTION BY SONOPORATION USING CATIONIC AND NEUTRAL MICROBUBBLES

Jose L. Tlaxca[*], **Christopher R. Anderson**[†], **Alexander L. Klibanov**[*,‡,§], **Bryce Lowrey**[*], **John A. Hossack**[*], **J. Steven Alexander**[¶], **Michael B. Lawrence**[*], and **Joshua J. Rychak**[†]

[*] Department of Biomedical Engineering, University of Virginia, Charlottesville, VA

[†] Targeson, Inc., San Diego, CA

[‡] Cardiovascular Research Center, University of Virginia, Charlottesville, VA

[§] Cardiovascular Division, Department of Internal medicine, University of Virginia, Charlottesville, VA

[¶] Department of Molecular and Cellular Physiology, Louisiana State University Health Science center, Shreveport, LA

Abstract

The objective of the study was to examine the role of acoustic power intensity and microbubble and plasmid concentrations on transfection efficiency in HEK-293 cells using a sonoporator with a 1-MHz transducer. A green fluorescent protein (GFP) reporter plasmid was delivered in as much as 80% of treated cells, and expression of the GFP protein was observed in as much as 75% of cells, using a power intensity of 2 W/cm^2 with a 25% duty cycle. In addition, the relative transfection abilities of a lipid noncationic and cationic microbubble platform were investigated. As a positive control, cells were transfected using Lipofectamine reagent. Cell survival and transfection efficiency were inversely proportional to acoustic power and microbubble concentration. Our results further demonstrated that high-efficiency transfection could be achieved, but at the expense of cell loss. Moreover, direct conjugation of plasmid to the microbubble did not appear to significantly enhance transfection efficiency under the examined conditions, although this strategy may be important for targeted transfection *in vivo*.

Keywords

Ultrasound; Sonoporation; Microbubble; Transfection efficiency; Gene delivery; Cationic micro bubbles

INTRODUCTION

One of the most significant unmet challenges in the field of gene therapy is the development of nontoxic and efficient delivery mechanisms. This problem exists at the clinical level and to some extent within experimental science as well. Gene delivery systems can be broadly divided into viral and nonviral systems (Nabel 1995). Viral vectors are generally the most efficient means of introducing therapeutic DNA into target cells (Robbins and Ghivizzani 1998) and oftentimes are able to mediate long-duration transgene expression (Burke et al.

Address correspondence to: Michael B. Lawrence, Ph.D., Associate Professor and Chair, Department of Biomedical Engineering, University of Virginia, MR-5 Building, Room 2111, P.O. Box 800759, Charlottesville, VA 22908. mbl2a@virginia.edu.
JJR and ALK report stock ownership in Targeson, Inc.

2002). However, immunotoxicity, insertional mutagenesis and lack of site specificity have been historical obstacles for this technology (Gallo-Penn et al. 2001; Marshall 1999). Nonviral transfection approaches include chemical techniques such as lipofection (Felgner and Ringold 1989), electrodynamic approaches such as electroporation and nucleofection (Neumann 1989), particle bombardment (also known as gene gun) (Klein et al. 1992) and acoustic-based methods such as sonoporation (Bao et al. 1997; Lawrie et al. 2000; Miller et al. 1999b; Ward et al. 1999, 2000). In the research setting, these nonviral methods are generally efficacious for most types of cultured cells and have shown some translatability to *in vivo* use. However, significant technical challenges remain to be solved.

We and others (Bekeredjian et al. 2003; Kinoshita and Hynynen 2005; Leong-Poi et al. 2007; Li et al. 2008; Mehier-Humbert et al. 2005; Meijering et al. 2007; Miller et al. 1999a; Otani et al. 2009; Rahim et al. 2006) have hypothesized that acoustically mediated sonoporation offers significant advantages in transfection efficiency, safety, cost and specificity over other technologies. The use of gas-encapsulated microbubbles (MBs) as gene delivery vehicles and transfection-enhancing agents is particularly promising. The presence of a MB in an acoustic field can transform the incident low-density acoustic energy into concentrated, high-density energy. This effect is a result of the compressibility of the MB, which undergoes vigorous oscillations in the acoustic field. These oscillations, which can be violent enough to cause fragmentation of the MB, result in a significant momentum transfer that can surpass the threshold for poration of the cell membrane and induction of endocytosis (Meijering et al. 2009). This phenomenon, known as *sonoporation*, has been demonstrated to mediate the transfer of both DNA and other macromolecules (Bao et al. 1997; Greenleaf et al. 1998; Guzman et al. 2001; Kim et al. 1996; Tata et al. 1997).

Sonoporation has been investigated as a noninvasive and low-cost technique, primarily for *in vivo* applications, although no clinical or research applications have yet been successfully commercialized. One reason for this may be the extreme diversity of acoustic, biological and MB variables in the reported studies of the sonoporation phenomenon (Forbes et al. 2008; Karshafian et al. 2009; Miller and Dou 2009; van Wamel et al. 2006). This makes it exceptionally difficult to draw specific conclusions regarding the efficacy of this technique, especially with respect to competing transfection methods. Confounding matters further is the widespread use of diagnostic MB agents marketed for clinical use, among which there are striking variations in particle size, shell stability and gas content. The absence of a definitive mechanistic explanation for the sonoporation effect, coupled with the absence of standardized MB preparations optimized for sonoporation, presents a significant barrier to the further development and commercialization of this promising technology.

In the present study, we explore the role of several variables of relevance to sonoporation in a carefully controlled and reproducible system, and compare the transfection efficiency of sonoporation with that of an established chemical transfection technique. We use a lipid MB along with a sonoporator, both of which are commercially available for research use. In addition, we explore the ability of cationically charged MBs to carry a nucleic acid payload, and compare the transfection efficiency of these MBs with conventional neutral MBs.

MATERIALS AND METHODS

Plasmids

A reporter plasmid coding for green fluorescent protein (GFP) was used in all studies. Expression in this plasmid (pmaxGFP; Amaxa Biosciences, Cologne, Germany) is driven by a cytomegalovirus promoter, and the plasmid has a molecular weight of 2300 kDa (3486 bp). The plasmid was amplified in Epicurian Coli XL10 gold ultracompetent cells (Stratagene, La Jolla, CA, USA) and then isolated and purified using QIAGEN plasmid giga

kit (Qiagen, Valencia, CA, USA) following the manufacturer's protocol. Plasmid concentration was assessed by photometric absorption at 260 nm.

Cell culture

Three adherent cell lines were examined in this study. b. End.3 (mouse brain endothelium), HEK-293 (human embryonic kidney) and SVEC4-10 (murine endothelial cell line derived by SV40 transformation) were purchased from ATCC (Manassas, VA, USA). SV-LEC, a mouse lymphatic endothelial cell line from the mesenteric adventitial tissue, was generated as described previously (Ando et al. 2005). b. END.3, SV-LEC and HEK-293 cells were maintained in Dulbecco modified eagle medium (DMEM; Invitrogen, Carlsbad, CA, USA) and supplemented with 10% (v/v) fetal bovine serum (FBS; Invitrogen) and 1% (v/v) penicillin/streptomycin (P/S; Invitrogen) in a 95% air-5% CO_2 humidified atmosphere at 37 °C. The SVEC4-10 cells were similarly maintained, except for the addition of 10% heat-inactivated FBS.

b.END.3, SVEC4-10 and SV-LEC cells were plated in treated 35-mm culture dishes (Corning, Corning, NY, USA) or OptiCell cartridges (Nalge Nunc International, Rochester, NY, USA) at a density of 1.5×10^5 cell/mL and incubated for 24 h before experimental treatment. HEK-293 cells were plated in OptiCells at a density of 2×10^5 cell/mL and incubated for 48 h before treatment. The Opti-Cell is a thin, acoustically transparent cartridge composed of two parallel sheets of gas-permeable polystyrene membrane with a thickness of 75 μm and surface area of 50 cm^2. The recommended fill volume of 10 mL was used in each OptiCell in this study. A plasmid DNA-MB mixture of known concentration was injected into the OptiCell, slowly inverting it five times before ultrasound treatment.

All cells were 70–80% confluent at the time of treatment. Cells were harvested 48 h after treatment with 0.05% (w/v) trypsin and 0.02% (w/v) ethylenediamine tetraacetic acid in Hank's balanced salt solution (HBSS) without calcium and magnesium. Unless otherwise stated, cells were centrifugally washed three times for 4 min at 400×*g* before determination of surviving cells by trypan-blue exclusion and hemacytometer analysis.

Microbubbles

Microbubbles used in this study were composed of a decafluorobutane core encapsulated by a lipid shell (Fig. 1a). Two MB formulations were examined in this study. TS-01-001, also known as Targestar-P (Targeson; San Diego, CA, USA) is a commercially available lipid-encapsulated decafluorobutane MB with an essentially neutral surface charge. The TS-02-008 preparation is a cationic MB platform, which is prepared by sonication of an aqueous dispersion of polyethyleneglycol-40 stearate (Sigma-Aldrich, St. Louis, MO, USA); 1, 2-dis-tearoyl-3-trimethylammoniumpropane (DTAP; Avanti, Alabaster, AL, USA); and disteroylphosphatidylcholine (DSPC, Avanti) in the presence of decafluorobutane, as described previously (Rychak et al. 2007). The inclusion of DTAP (2% by molarity) in TS-02-008 imparted the agent with a slight net positive surface charge (Christiansen et al. 2003). A small amount of biotin-polyethyleneglycol-40 stearate (PEG)-distearoylphospha tidylethanolamine was included in the TS-02-008 preparation for the purpose of conjugating a targeting ligand to the bubble surface, which will be presented in a subsequent publication. Microbubble concentration and size distribution was assessed by electrozone sensing using a Coulter Multisizer 4 (Beckman-Coulter, Miami, FL, USA).

Plasmid conjugation to cationic MBs

Cationic MBs were diluted to a concentration of ~1×10^8 in sterile 0.9% saline, and incubated with the pmaxGFP plasmid for 25 min at room temperature, with occasional shaking to redisperse the MBs. After incubation, unbound plasmid was removed by two

rounds of centrifugal washing for 5 min at 400×*g* in 5 mL of phosphate-buffered saline (PBS), and resuspended in 0.5 mL of PBS. For the plasmid-bearing MB characterization, the plasmid was labeled with the nucleotide-avid fluorophore YOYO-1 or TOTO-3 (Molecular Probes, Eugene, OR, USA) as follows. Fluorophore was incubated with the plasmid-conjugated MB dispersion at 3 μg per 1×10^8 MBs for 25 min at room temperature, and unbound fluorophore was removed by two rounds of centrifugal washing. Microbubbles were then counted and resuspended in PBS at a final concentration of 1×10^7 MB/mL for subsequent analysis or transfection experiments.

Sonoporation

The experimental transfection setup used in this study is shown in Fig. 1b. A commercially available sonoporator, model SP100 (Sonidel Ltd., Dublin, Ireland), was used for all experiments. This unit consists of a hand-held piezoelectric transducer with a center frequency of 1 MHz. The power intensity (measured in W/cm^2), duty cycle (% of full) and insonation time on this unit are controllable by the user. The beam characteristics of the transducer used in this study were measured as follows. A PVDF bilaminar membrane hydrophone (GEC Marconi Research Centre GL-0085, Essex, UK) was mounted in a water bath, and the position of the transducer relative to the hydrophone (50-mm distance) was controlled using a motorized stage (Newport Research Corp, Irvine, CA, USA). Acoustic pressures were measured in 0.5-mm steps along the transducer width, covering a total distance of 19 mm, spanning beyond the diameter (d = 16 mm) of the transducer.

For all experiments, the OptiCell containing the target cells was mounted horizontally in a heated bath (37 °C) of deionized water, with the cell monolayer on the upper surface of the OptiCell. The transducer was hand-held in the bath 50 mm below the OptiCell cell culture monolayer. A second OptiCell with a single acoustic transparent membrane was used as a guide to maintain the correct separation distance (see Fig. 1b). When the transducer was closer than 50 mm, there was high cell detachment (70%). The power intensity ranged from 0.3–5.0 W/cm^2. Unless otherwise stated, the duty cycle and insonation time for all experimental conditions were 25% and 3 min, respectively. The transducer was translated manually across the surface of the OptiCell at approximately 60 mm/s to evenly cover the entire area, corresponding to 35-s insonation time per cell. Microbubble and plasmid concentrations reported here represent the final concentration in the 10-mL OptiCell chamber. Transfection efficiencies reported here represent the fraction of cells recovered at 48 h post treatment. For the time course of intracellular delivery of plasmid, cells were harvested at 0, 4, 12, 24 and 48 h after treatment.

Cell viability and flow cytometry analysis

After sonoporation treatment, cells were removed from the OptiCell by trypsinization, collected by centrifugation and washed three times with HBSS, then counted and resuspended in binding buffer (10mM HEPES [4-(2-hydroxyethyl)-1-piperazineethanesulfonic acid]/NaHO, pH 7.4, 140 mM NaCl and 2.5 mM $CaCl_2$) at a concentration of 1×10^5 cells/mL. The number of intact cells recovered after treatment was determined by trypan blue exclusion and hemacytometer counting. The viability of surviving cells was measured by staining with fluorescently labeled Annexin V (AV) and 7-amino-actinomycin (7-AAD) (BD Pharmingen, San Diego, CA, USA). Five μL each of AV and 7-AAD conjugate were added to 100 μL of the cell suspension and incubated for 15 min at room temperature in the dark. After incubation, 400 μL of binding buffer was added. Single stain-positive control samples used to determine compensation and quadrants were prepared as follows: HEK-293 cells were killed by 10-min treatment in a 70 °C water bath and subsequently stained with AV or 7-AAD alone. All samples were analyzed by flow cytometry within 1 h. GFP, AV and 7-AAD expressions were analyzed using a

FACSCalibur system (Becton-Dickinson, Franklin Lakes, NJ, USA). Cells that were (+/−) AV/7-AAD were considered to be viable, (−/+) AV/7-AAD were considered apoptotic and (−/−) AV/7-AAD were end-stage apoptotic or necrotic cells.

Flow cytometry was also used to examine the conjugation of fluorescently labeled plasmid to MBs. Micro-bubbles were diluted to 5×10^6 MB/mL in PBS before flow cytometry, and a minimum of 50,000 gated events were collected. Microbubbles were gated in a forward *versus* side scatter dot plot (Fig. 2a), as previously described (Lindner et al. 2001;Rychak et al. 2005). All flow cytometry data were analyzed with FLOWjo Software (http://www.treestar.com/flowjo).

Statistical analysis

All data are expressed as mean ± standard deviation (SD), unless otherwise noted. All differences were evaluated by using the two-tailed Student's *t*-test, with $p < 0.05$ considered statistically significant. Unless otherwise stated, each independent sample consists of one OptiCell.

RESULTS

Microbubble characterization and coupling assessment

Plasmid conjugation to neutral and cationic MBs was determined spectrophotometrically and by flow cytometry. A sigmoid forward-side scatter plot, characteristic of polydisperse gas-encapsulated MBs, was observed by flow cytometry (Fig. 2a). A strong fluorescence signal was observed for YOYO-1–labeled plasmid incubated with cationic, but not neutral, MBs (Fig. 2b). Colocalization of fluorescently labeled plasmid to MBs was revealed by epifluorescence microscopy (Fig. 2c), with its corresponding same field of view brightfield image (Fig. 2d). Quantitation of MB-bound plasmid by spectrophotometric measurements at 260/280 nm revealed a maximum plasmid payload of 8 μg and 2.9 μg per 10^8 MB for cationic and neutral MBs, respectively (Fig. 2e). The mean diameter of cationic and neutral MBs was 2.98 and 2.89 μm, respectively, as measured by electrozone sensing with a Coulter counter (Fig. 2f).

Acoustic characterization

Table 1 shows −6 dB beam widths as a function of power intensity, with a fixed 25% duty cycle, measured at 50 mm from the transducer face. The beam width decreased from 14.4 mm to 12 mm with increasing power intensity, 0.3–5.0 W/cm^2. The SP100 device produced a pulse repetition frequency (PRF) of 100 Hz and 2.5-ms pulse duration with a center frequency of 1 MHz (data not shown).

Transfection and viability

Cells were transfected by sonoporating at 2 W/cm^2, 3.2 μg/mL plasmid and 4×10^7 MB/mL. As a positive control, cells were transfected with Lipofectamine 2000 (Invitrogen), a widely used chemical transfection reagent. Similar GFP level expression was observed by flow cytometry for cells transfected by sonoporation and Lipofectamine (Fig. 3a). Viability was measured by flow cytometry and trypan blue exclusion on cells that were not lysed and disintegrated because of the mechanical action of cavitation activity. Untreated, healthy stained cells exhibited low levels of AV and 7-AAD, as shown in Fig 3b. On average, 25% and 30% of the total number of recovered cells were apoptotic/necrotic after Lipofectamine or ultrasound treatment, respectively (Fig. 3c, 3d). Trypan blue dye exclusion, performed after three centrifugal washes, revealed a consistent level of necrosis at 10%, regardless of sonoporator settings, MB concentration or plasmid concentration (data not shown). Flow cytometry was judged to be more reproducible and enable higher experimental throughput

than the trypan blue exclusion method, and was used in all subsequent experiments (Table 2).

Intracellular delivery of plasmid by sonoporation

We used epifluorescence microscopy and flow cytometry to examine the time course of internalization and localization of delivered plasmid (Fig. 4). HEK-293 cells and neutral MBs were used in this experiment set. Plasmid was labeled with TOTO-3, a fluorophore that exhibited no spectral overlap with GFP by flow cytometry (data not shown). Low-level background fluorescence was observed on untreated cells (Fig. 4a). Cells treated at 2 W/cm^2, 3 min, 4×10^7 MB/mL with 3.2 μg/mL plasmid showed a clear increase in GFP intensity (Fig. 4b). The observed fluorescence signal spanned three decades of intensity, indicating a significant range in the brightness of transfected cells. Cells were harvested at 0, 4,12, 24 or 48 h post treatment and analyzed by flow cytometry and epifluorescence microscopy for GFP (expression of transfected protein) and TOTO-3 (presence of plasmid). As a control, a subset of cells was transfected with unlabeled plasmid. The red fluorescence emitted from TOTO-3 was consistently found in more than 80% of cells (Fig. 4c), and this did not substantially change over the 48-h time course examined here. GFP expression increased steadily over the 48-h period. Staining the plasmid with TOTO-3 did not appear to alter the expression of GFP (data not shown). Epifluorescence microscopy also revealed that the majority of cells appeared to take up the plasmid (Fig. 4d), although the resolution of the microscopy technique used here did not enable identification of the delivered plasmids' intracellular location.

Transfection efficiency and recovery

Microbubbles introduced into the OptiCell appeared as a cloudy white dispersion that gradually settled on the cell monolayer. Destruction of MBs, resulting in loss of opacity, was observed under all experimental treatments. The effects of ultrasound power intensity, MB concentration and plasmid DNA concentration were investigated using neutral MBs. Plasmid was added directly to the OptiCell, and the final concentration in the 10-mL Opti-Cell is reported here. HEK-293 cells were used for these experiments because of their robustness and general amenability to transfection. The number of recovered cells was measured by hemacytometer counting, and the viability of the recovered cells was measured by flow cytometric analysis of AV and 7-AAD.

There was a marked increasing trend in transfection efficiency at power intensity between 1 and 2 W/cm^2, and no change as power intensity was increased above 2 W/cm^2 (Fig. 5a). The mechanical index (MI) is defined as the peak negative pressure divided by the square root of the center frequency of the beam. A five-fold decrease in recovered cell concentration, from approximately 14 million to 3 million cells per OptiCell, was observed at the range of 1–2 W/cm^2 (equivalent to a MI of 0.22 and 0.30). The threshold behavior observed at 1–2 W/cm^2 power intensity may be caused by the conversion from low-amplitude oscillation to high-amplitude nonlinear oscillation of the MBs, which is known to occur at a MI of 0.3–0.6 for agents similar to those investigated here (Chomas et al. 2001). However, the specific oscillatory behavior of the MBs could not be observed in the current experimental system. No change in the viability of recovered cells was observed as a function of power intensity. OptiCells were treated at a MB dose of 4×10^7 MB/mL with 3.2 μg/mL of plasmid.

Unlike the trend observed for power intensity, transfection efficiency appeared to scale linearly with MB concentration (Fig. 5b). A reduction in the number of recovered cells proportional to the MB concentration was observed, and no saturation behavior was observed over the range of MB concentrations examined here. A decrease in the viability of

recovered cells was observed with increasing MB concentration. Opticells in this experimental set were insonated at 2 W/cm^2 with 0.4 μg/mL of plasmid.

Increasing the plasmid concentration resulted in an increase in transfection efficiency, with a maximum of ~70% efficiency occurring at about 3 μg/mL plasmid. No reproducible trend in cell survival or cell viability was observed as a function of plasmid concentration (Fig. 5c). These experiments were performed at a MB dose of 4×10^7 MB/mL and power intensity of 2 W/cm^2.

Comparison of transfection efficiency

To explore the effect of direct conjugation of the plasmid to the MB surface, we compared the transfection efficiency of plasmid-loaded cationic MBs to that of neutral MBs (Fig. 6). Cationic or neutral MBs were incubated with 8 μg plasmid per 10^8 MB, and then washed three times to remove unbound plasmid. These incubation conditions resulted in approximately 6 and 2 μg of plasmid per 10^8 MB (Fig. 2e). In addition, some cells were treated with neutral MBs plus 8 μg plasmid per 10^8 MB without washing, resulting in approximately the same effective plasmid concentration as the plasmid-loaded cationic MB. The same concentration of MBs was added to each OptiCell (4×10^7 MB/mL), and all samples were sonoporated at 2.0 W/cm^2 for 3 min. Measurement of GFP expression performed 48 h after treatment by flow cytometry revealed a transfection efficiency of ~65% using neutral MBs plus plasmid (8 μg per 10^8 MB, free in solution). Treatment with cationic MBs loaded with 6 μg per 10^8 MB resulted in a °70% transfection efficiency, and neutral MBs from which the majority of conjugated plasmid had been removed by washing resulted in less than 10% transfection (Fig. 6a). Direct conjugation of the plasmid to the cationic MB surface did not appreciably increase transfection efficiency relative to cells treated with neutral MBs plus an equal quantity of unconjugated plasmid.

The transfection efficiency of neutral and plasmid-loaded cationic MBs was then compared with that of Lipofectamine-2000 for various adherent cell lines. In general, cationic MBs loaded with 3.2 μg/mL plasmid resulted in a slight increase in transfection efficiency with respect to neutral MBs plus 3.2 μg/mL free plasmid; this effect was statistically significant only for HEK-293 cells. The transfection efficiency of plasmid-loaded cationic MBs was statistically identical to that achieved by Lipofectamine-2000 for all cell types examined except SV-LEC (Fig. 6b).

DISCUSSION

In this study, we have explored the ability of MB-based sonoporation to mediate transfection *in vitro* using a reproducible and readily implemented experimental system. We used flow cytometry and fluorescence microscopy to examine (i) the time course of plasmid delivery and (ii) the role of several user-adjustable sonoporation parameters on transfection efficiency and cell recovery and viability. In addition, we investigated the feasibility of conjugation of plasmid DNA to the MB surface. We observed an inverse relationship between transfection efficiency and cell recovery. As much as 80% of recovered cells received plasmid, and a maximum transfection efficiency of 70% was observed. Plasmid was conjugated to the surface of cationic MBs, although direct plasmid conjugation to the MB did not significantly increase transfection efficiency in our experimental setup.

We observed several interesting phenomena in our *in vitro* sonoporation system. Transfection efficiency scaled with plasmid concentration, and saturated at approximately 3 μg per mL of medium volume. This is equivalent to an average of ~1.4×10^6 plasmid copies per cell, resulting in ~70% transfection efficiency (Fig. 5c), which is the same order of magnitude reported in Tseng et al. (1997). We observed no change in either cell recovery or

toxicity over plasmid doses between 0 and 6.4 μg/mL. Transfection efficiency increased approximately linearly with MB concentration, and cell recovery correlated inversely with concentration. A decreasing cell viability trend was observed as a function of increasing MB concentration. No transfection was observed in the absence of MBs. The relationship between acoustic power and transfection efficiency was highly nonlinear. Transfection efficiency increased sharply between 1 and 2.0 W/cm^2, and cell recovery showed a similarly sharp decrease. Above 2.0 W/cm^2, no change in either transfection efficiency or cell recovery and no significant change in cell viability as a function of acoustic power were noted and remained about 70% for all experimental conditions. It is known that MBs can experience violent expansion and compression at the highest pressures used in this experiment, which results in destruction or fragmentation of the shell (Hernot and Klibanov 2008). We presume that this highly focused energy may be responsible for the observed destruction of adjacent cells.

The results presented here and elsewhere (Bao et al. 1997; Karshafian et al. 2009; Zarnitsyn and Prausnitz 2004) have demonstrated what appears to be a critical limitation of sonoporation: transfection efficiency appears to be proportional to cell death. We have found that high transfection efficiencies (>95% in some individual cases) can be achieved, although at the expense of significant cell death. This trend appears strongly dependent on acoustic power and MB concentration, which suggests that both sonoporation and cell death are related to nonlinear MB oscillation and/or destruction at high power. Cell death appears to be primarily the result of mechanical disintegration, and significant cavitation activity is known to occur from high-amplitude MB oscillation. Clearly, treatment protocols in which sonoporation is high but cell death is low are desired, and this represents a clear near-term goal in the further development of this technology. Careful tuning of the acoustic pressure, MB concentration and pulsing sequence may enable high-efficiency transfection with minimum cell death.

We have demonstrated that incubation of plasmid DNA with lipid MBs results in a measurable conjugation. This effect was greatest for the cationic MBs, although noncharged MBs also appeared too complex with small quantities of plasmid. Spectrophotometry indicated a saturating concentration of 8 μg per 1×10^8 cationic MBs, and flow cytometry and fluorescent microscopy suggest that every cationic MB has some plasmid coupled to its shell at this condition. Based on the plasmid size (3490 base pairs), this translates into an average of 20,942 plasmids per MB, which is on the same order of magnitude as found in previous studies using a similar MB system (Christiansen et al. 2003; Haag et al. 2006).

Our data demonstrate that direct conjugation of the plasmid to the MB does not generally result in increased transfection efficiency, provided that a relatively high plasmid concentration in the bulk fluid can be maintained. Our *in vitro* system is static, and free plasmid added to the system can be assumed to distribute evenly. *In vivo*, however, achieving a suitably high systemic concentration may be impossible or unsafe; thus, we hypothesize that loading of the plasmid to the MB may be critical to enabling high-efficiency transfection *in vivo*. In addition, the direct loading of the MB with the plasmid enables the possibility of site-targeted transfection, which we will explore in a subsequent study.

We used the chemical transfection reagent Lipofectamine as a gold standard in the study presented here. Lipofectamine and similar products are perhaps the easiest and most widely-used benchtop transfection technology, although electroporation-type methods are generally thought to mediate higher transfection efficiencies. Numerous other methods are in commercial operation, each with individual strengths and weaknesses. Chemical type methods work very well with a subset of robust cell types, although they offer limited

control of spatial and temporal specificity (Gershon et al. 1993). Electroporation uses high-voltage electric fields to create cell membrane pores. This can allow some control over the spatial extent of transfection, although the electroporation process is invasive and can cause significant cell death (Chang and Reese 1990; Yamashita et al. 2002). Particle bombardment is a mechanical transfection technique that uses subcellular-sized particles coated with genes that are made to penetrate the membrane at high velocity (Williams et al. 1991; Yang et al. 1990; Zelenin et al. 1989) but appears to be limited to surface (*i.e.*, skin) applications (Miller et al. 2002).

The sonoporation phenomenon investigated here is a nonviral transfection technique that uses MBs and ultrasound. We hypothesize that this technique may be applied as a low-cost and potentially high-efficiency technique for rapidly transfecting cultured cells *in vitro*. In particular, transfection of cells generally resistant to transfection by competing methods may be a unique application. Specific localization of transfection can, in theory, be achieved by the use of targeted MBs or focused ultrasound, although this has not yet been demonstrated *in vivo*. Ultrasound generally does not suffer from tissue depth-dependent effects as with electroporation and gene guns, although transfection of bone and gas-containing structures (lungs) are likely not to be feasible because of severe attenuation effect. The MBs contemplated here as gene delivery vehicles are confined to the intravascular compartment because of their micron-scale diameter. Thus, targeted transfection of endothelial or perivascular tissue may be possible, but reaching deeper tissue layers may be difficult without disruption of the endothelial wall barrier. However, the vascular endothelium may be an ideal target for gene therapy in the context of inflammatory disease, because down-regulating the pro-inflammatory cell surface molecules may serve to modulate leukocyte recruitment and subsequent inflammation. The cells explored in the current study, with the exception of HEK-293, are of an endothelial phenotype and enabled us to carefully assess the feasibility of transfection *in vitro* using a model genetic payload.

It was found that, under various conditions of acoustic power intensity and MB concentration, cell recovery and transfection efficiency are inversely proportional. The results presented here demonstrate that high efficiency can be achieved, although effort directed at minimizing cell loss is still needed. The lack of flow is a major limitation in our experimental system; direct conjugation of the plasmid to the MB did not enhance transfection efficiency, although this strategy might be important in a targeted gene delivery system where shear forces are significantly higher.

Acknowledgments

The authors gratefully acknowledge the assistance and advice of Linsey C. Phillips and are grateful for equipment support from Artison, Inc. and Sonidel, LTD. This work was supported by the NIH Bioengineering Research Partnership (BRP) EB002185 (to M.B.L.) and 1R43DK079406-01 by the National Institute of Diabetes and Digestive and Kidney Diseases (NIDDK) (to J.J.R.).

References

Ando T, Jordan P, Joh T, Wang Y, Jennings MH, Houghton J, Alexander JS. Isolation and characterization of a novel mouse lymphatic endothelial cell line: SV-LEC. Lymphat Res Biol 2005;3:105–115. [PubMed: 16190815]

Bao S, Thrall BD, Miller DL. Transfection of a reporter plasmid into cultured cells by sonoporation in vitro. Ultrasound Med Biol 1997;23:953–959. [PubMed: 9300999]

Bekeredjian R, Chen S, Frenkel PA, Grayburn PA, Shohet RV. Ultrasound-targeted microbubble destruction can repeatedly direct highly specific plasmid expression to the heart. Circulation 2003;108:1022–1026. [PubMed: 12912823]

Burke B, Sumner S, Maitland N, Lewis CE. Macrophages in gene therapy: Cellular delivery vehicles and in vivo targets. J Leukoc Biol 2002;72:417–428. [PubMed: 12223508]

Chang DC, Reese TS. Changes in membrane structure induced by electroporation as revealed by rapid-freezing electron microscopy. Biophys J 1990;58:1–12. [PubMed: 2383626]

Chomas JE, Dayton P, Allen J, Morgan K, Ferrara KW. Mechanisms of contrast agent destruction. IEEE Trans Ultrason Ferroelectr Freq Control 2001;48:232–248. [PubMed: 11367791]

Christiansen JP, French BA, Klibanov AL, Kaul S, Lindner JR. Targeted tissue transfection with ultrasound destruction of plasmid-bearing cationic microbubbles. Ultrasound Med Biol 2003;29:1759–1767. [PubMed: 14698343]

Felgner PL, Ringold GM. Cationic liposome-mediated transfection. Nature 1989;337:387–388. [PubMed: 2463491]

Forbes MM, Steinberg RL, O'Brien WD Jr. Examination of inertial cavitation of Optison in producing sonoporation of chinese hamster ovary cells. Ultrasound Med Biol 2008;34:2009–2018. [PubMed: 18692296]

Gallo-Penn AM, Shirley PS, Andrews JL, Tinlin S, Webster S, Cameron C, Hough C, Notley C, Lillicrap D, Kaleko M, Connelly S. Systemic delivery of an adenoviral vector encoding canine factor VIII results in short-term phenotypic correction, inhibitor development, and biphasic liver toxicity in hemophilia A dogs. Blood 2001;97:107–113. [PubMed: 11133749]

Gershon H, Ghirlando R, Guttman SB, Minsky A. Mode of formation and structural features of DNA-cationic liposome complexes used for transfection. Biochemistry 1993;32:7143–7151. [PubMed: 8343506]

Greenleaf WJ, Bolander ME, Sarkar G, Goldring MB, Greenleaf JF. Artificial cavitation nuclei significantly enhance acoustically induced cell transfection. Ultrasound Med Biol 1998;24:587–595. [PubMed: 9651968]

Guzman HR, Nguyen DX, Khan S, Prausnitz MR. Ultrasound-mediated disruption of cell membranes. II. Heterogeneous effects on cells. J Acoust Soc Am 2001;110:597–606. [PubMed: 11508985]

Haag P, Frauscher F, Gradl J, Seitz A, Schafer G, Lindner JR, Klibanov AL, Bartsch G, Klocker H, Eder IE. Microbubble-enhanced ultrasound to deliver an antisense oligodeoxynucleotide targeting the human androgen receptor into prostate tumours. J Steroid Biochem Mol Biol 2006;102:103–113. [PubMed: 17055720]

Hernot S, Klibanov AL. Microbubbles in ultrasound-triggered drug and gene delivery. Adv Drug Deliv Rev 2008;60:1153–1166. [PubMed: 18486268]

Karshafian R, Bevan PD, Williams R, Samac S, Burns PN. Sonoporation by ultrasound-activated microbubble contrast agents: Effect of acoustic exposure parameters on cell membrane permeability and cell viability. Ultrasound Med Biol 2009;35:847–860. [PubMed: 19110370]

Kim HJ, Greenleaf JF, Kinnick RR, Bronk JT, Bolander ME. Ultrasound-mediated transfection of mammalian cells. Hum Gene Ther 1996;7:1339–1346. [PubMed: 8818721]

Kinoshita M, Hynynen K. A novel method for the intracellular delivery of siRNA using microbubble-enhanced focused ultrasound. Biochem Biophys Res Commun 2005;335:393–399. [PubMed: 16081042]

Klein RM, Wolf ED, Wu R, Sanford JC. High-velocity microprojectiles for delivering nucleic acids into living cells. 1987. Biotechnology 1992;24:384–386. [PubMed: 1422046]

Lawrie A, Brisken AF, Francis SE, Cumberland DC, Crossman DC, Newman CM. Microbubble-enhanced ultrasound for vascular gene delivery. Gene Ther 2000;7:2023–2027. [PubMed: 11175314]

Leong-Poi H, Kuliszewski MA, Lekas M, Sibbald M, Teichert-Kuliszewska K, Klibanov AL, Stewart DJ, Lindner JR. Therapeutic arteriogenesis by ultrasound-mediated VEGF165 plasmid gene delivery to chronically ischemic skeletal muscle. Circ Res 2007;101:295–303. [PubMed: 17585071]

Li YS, Reid CN, McHale AP. Enhancing ultrasound-mediated cell membrane permeabilisation (sonoporation) using a high frequency pulse regime and implications for ultrasound-aided cancer chemotherapy. Cancer Lett 2008;266:156–162. [PubMed: 18367324]

Lindner JR, Song J, Christiansen J, Klibanov AL, Xu F, Ley K. Ultrasound assessment of inflammation and renal tissue injury with microbubbles targeted to P-selectin. Circulation 2001;104:2107–2112. [PubMed: 11673354]

Marshall E. Gene therapy death prompts review of adenovirus vector. Science 1999;286:2244–2245. [PubMed: 10636774]

Mehier-Humbert S, Bettinger T, Yan F, Guy RH. Ultrasound-mediated gene delivery: Kinetics of plasmid internalization and gene expression. J Control Release 2005;104:203–211. [PubMed: 15866346]

Meijering BD, Henning RH, Van Gilst WH, Gavrilovic I, Van Wamel A, Deelman LE. Optimization of ultrasound and microbubbles targeted gene delivery to cultured primary endothelial cells. J Drug Target 2007;15:664–671. [PubMed: 18041634]

Meijering BD, Juffermans LJ, van Wamel A, Henning RH, Zuhorn IS, Emmer M, Versteilen AM, Paulus WJ, van Gilst WH, Kooiman K, de Jong N, Musters RJ, Deelman LE, Kamp O. Ultrasound and microbubble-targeted delivery of macromolecules is regulated by induction of endocytosis and pore formation. Circ Res 2009;104:679–687. [PubMed: 19168443]

Miller DL, Bao S, Gies RA, Thrall BD. Ultrasonic enhancement of gene transfection in murine melanoma tumors. Ultrasound Med Biol 1999a;25:1425–1430. [PubMed: 10626630]

Miller DL, Bao S, Morris JE. Sonoporation of cultured cells in the rotating tube exposure system. Ultrasound Med Biol 1999b;25:143–149. [PubMed: 10048811]

Miller DL, Dou C. Induction of apoptosis in sonoporation and ultrasonic gene transfer. Ultrasound Med Biol 2009;35:144–154. [PubMed: 18723272]

Miller DL, Pislaru SV, Greenleaf JE. Sonoporation: mechanical DNA delivery by ultrasonic cavitation. Somat Cell Mol Genet 2002;27:115–134. [PubMed: 12774945]

Nabel EG. Gene therapy for cardiovascular disease. Circulation 1995;91:541–548. [PubMed: 7805260]

Neumann, E. The relaxation hysteresis of membrane electroporation. In: Neumann, E.; Sowers, AE.; Jordan, CA., editors. Electroporation and electrofusion in cell biology. New York: Plenum Press; 1989. p. 61-82.

Otani K, Yamahara K, Ohnishi S, Obata H, Kitamura S, Nagaya N. Nonviral delivery of siRNA into mesenchymal stem cells by a combination of ultrasound and microbubbles. J Control Release 2009;133:146–153. [PubMed: 18976686]

Rahim A, Taylor SL, Bush NL, ter Haar GR, Bamber JC, Porter CD. Physical parameters affecting ultrasound/microbubble-mediated gene delivery efficiency in vitro. Ultrasound Med Biol 2006;32:1269–1279. [PubMed: 16875960]

Robbins PD, Ghivizzani SC. Viral vectors for gene therapy. Pharmacol Ther 1998;80:35–47. [PubMed: 9804053]

Rychak JJ, Klibanov AL, Hossack JA. Acoustic radiation force enhances targeted delivery of ultrasound contrast microbubbles: In vitro verification. IEEE Trans Ultrason Ferroelectr Freq Control 2005;52:421–433. [PubMed: 15857050]

Rychak JJ, Klibanov AL, Ley KF, Hossack JA. Enhanced targeting of ultrasound contrast agents using acoustic radiation force. Ultrasound Med Biol 2007;33:1132–1139. [PubMed: 17445966]

Tata DB, Dunn F, Tindall DJ. Selective clinical ultrasound signals mediate differential gene transfer and expression in two human prostate cancer cell lines: LnCap and PC-3. Biochem Biophys Res Commun 1997;234:64–67. [PubMed: 9168961]

Tseng WC, Haselton FR, Giorgio TD. Transfection by cationic liposomes using simultaneous single cell measurements of plasmid delivery and transgene expression. J Biol Chem 1997;272:25641–25647. [PubMed: 9325286]

van Wamel A, Kooiman K, Harteveld M, Emmer M, ten Cate FJ, Versluis M, de Jong N. Vibrating microbubbles poking individual cells: Drug transfer into cells via sonoporation. J Control Release 2006;112:149–155. [PubMed: 16556469]

Ward M, Wu J, Chiu JF. Ultrasound-induced cell lysis and sonoporation enhanced by contrast agents. J Acoust Soc Am 1999;105:2951–2957. [PubMed: 10335644]

Ward M, Wu J, Chiu JF. Experimental study of the effects of Optison concentration on sonoporation in vitro. Ultrasound Med Biol 2000;26:1169–1175. [PubMed: 11053752]

Williams RS, Johnston SA, Riedy M, DeVit MJ, McElligott SG, Sanford JC. Introduction of foreign genes into tissues of living mice by DNA-coated microprojectiles. Proc Natl Acad Sci U S A 1991;88:2726–2730. [PubMed: 2011582]

Yamashita Y, Shimada M, Tachibana K, Harimoto N, Tsujita E, Shirabe K, Miyazaki J, Sugimachi K. In vivo gene transfer into muscle via electro-sonoporation. Hum Gene Ther 2002;13:2079–2084. [PubMed: 12490002]

Yang NS, Burkholder J, Roberts B, Martinell B, McCabe D. In vivo and in vitro gene transfer to mammalian somatic cells by particle bombardment. Proc Natl Acad Sci U S A 1990;87:9568–9572. [PubMed: 2175906]

Zarnitsyn VG, Prausnitz MR. Physical parameters influencing optimization of ultrasound-mediated DNA transfection. Ultrasound Med Biol 2004;30:527–538. [PubMed: 15121255]

Zelenin AV, Titomirov AV, Kolesnikov VA. Genetic transformation of mouse cultured cells with the help of high-velocity mechanical DNA injection. FEBS Lett 1989;244:65–67. [PubMed: 2924911]

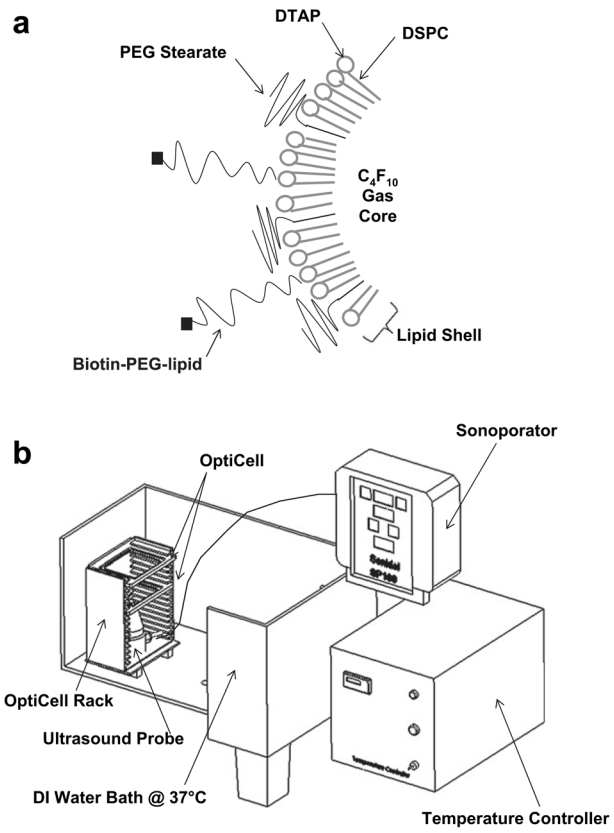

Fig. 1.

Experimental setup for transfection by sonoporation. (a) Schematic of MBs used in this experiment. Microbubbles were composed of a perfluorocarbon gas core encapsulated by a lipid and PEG-stearate shell. Cationic MBs contained a small amount of positively charged DTAP lipid and biotin-PEG-lipid. (b) Cell monolayers were cultured in 10 mL OptiCells, and MBs and plasmid were injected and mixed immediately before ultrasound treatment. The ultrasound transducer was hand-held in the heater water bath 50 mm below the OptiCell cell culture monolayer. A second OptiCell was used as a guide to maintain the correct separation distance of 50 mm. Buoyancy caused the MBs to rest against the cell monolayer in upper OptiCell membrane.

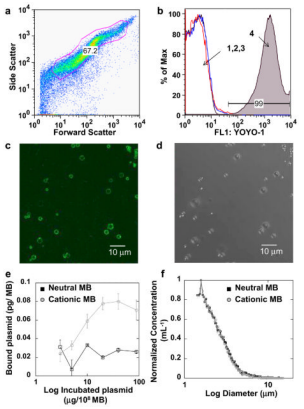

Fig. 2.

Plasmid conjugation to MB surface. Plasmid DNA was electrostatically coupled to the cationic MBs and subsequently labeled with YOYO-1. (a) Forward *vs.* side scatter of cationic MBs bearing plasmid labeled with YOYO-1, with gate showing the population of MBs analyzed. (b) Fluorescence histogram for (1) naked cationic MBs, (2) naked cationic MBs incubated with YOYO-1 and (3) neutral MBs incubated with plasmid and YOYO-1 showed low signal, whereas (4) cationic MBs incubated with plasmid and YOYO-1 showed a significant fluorescence signal. (c) Epifluorescent and (d) corresponding bright field microscopy showed co-localization of YOYO-1–stained plasmid with cationic MBs. (e) Photometric quantification of plasmid per MB, for both neutral and cationic MBs. (f) Microbubble size and normalized concentration.

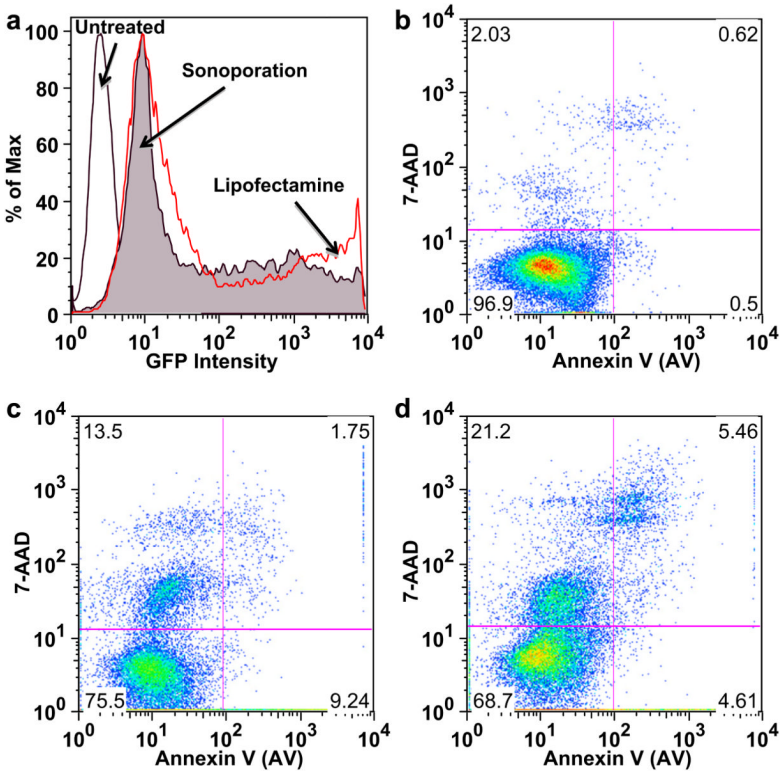

Fig. 3.

Flow cytometric analysis of HEK-293 viability and GFP expression. (a) Characteristic GFP intensity histogram on viable HEK-293 cells showing (1) minimal background fluorescence for untreated cells (*unfilled black curve*); (2) GFP expression in cells treated by Lipofectamine (*open red curve*); and (3) sonoporation with MBs (*filled curve*). Characteristic viability plots: (b) untreated healthy stained cells, (c) Cells transfected with pMax-GFP by Lipofectamine-2000 or (d) by sonoporation with MBs (2.0 W/cm^2, duty cycle of 25%, 4×10^7 neutral MBs per mL and 3.2 μg/mL of pMax-GFP plasmid).

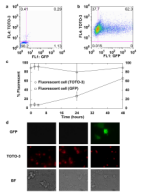

Fig. 4.

Time course of plasmid delivery and transfection. (a) Characteristic dot plot of untreated cells and (b) cells 48 h after treatment. (c) GFP (*squares*) and TOTO-3 (*circles*) signal measured by flow cytometry as a function of time after sonoporation treatment. (d) Characteristic epifluorescence and corresponding brightfield microscopy images of sonoporated cells at various time points: 0, 4 and 12 h, respectively. Data shown as mean ± standard deviation of Opticells ($n = 4$). HEK-293 cells were sonoporated at 2.0 W/cm^2, duty cycle of 25%, for 3 min with 4×10^7 neutral MBs per mL and 3.2 μg/mL of pMax-GFP plasmid labeled with TOTO-3 for all sonoporation experiments presented here.

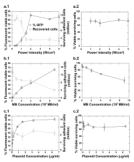

Fig. 5.

Transfection efficiency, recovery and viability as a function of sonoporation parameters. HEK-293 cells were incubated with neutral MBs and plasmid at the indicated concentrations, sonoporated for 3 min at 1.0 MHz and a duty cycle of 25% and assessed by flow cytometry 48 h post treatment. (a) Variable power intensity: cells were incubated with 3.2 μg/mL plasmid DNA and 4×10^7 MB/mL. (b) Variable MB concentration: cells were insonated at 2 W/cm^2 with 0.4 μg/mL plasmid. (c) Variable plasmid concentration: cells were incubated with 4×10^7 MB/mL and insonated at 2 W/cm^2. Data shown as mean ± standard deviation of OptiCells (n = 4).

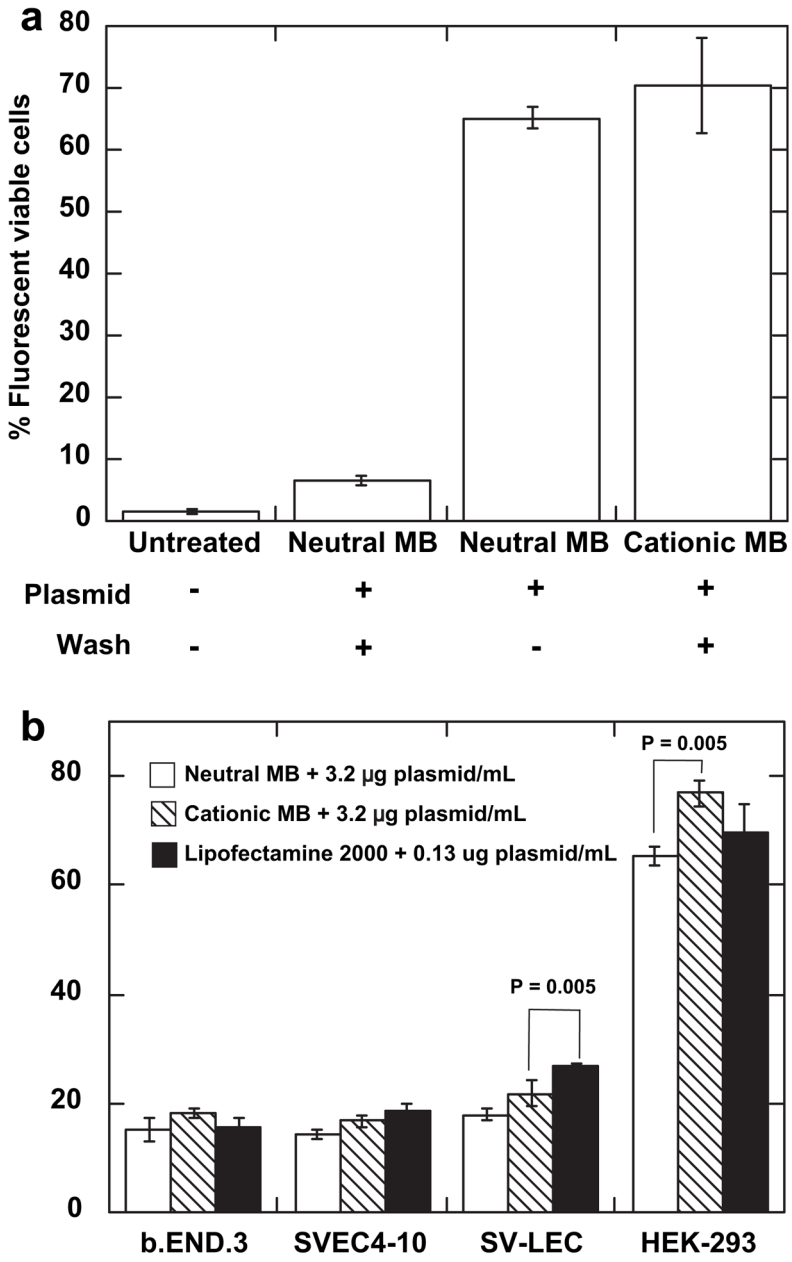

Fig. 6.

Transfection efficiency comparison. A MB concentration of 4×10^7 MB/mL was used for each experiment. Cells were insonated at 2.0 W/cm^2 for 3 min at a duty cycle of 25% and then harvested 48 h post-treatment and analyzed by flow cytometry. (a) Neutral and cationic MBs were incubated with 8 μg of pmaxGFP plasmid per 10^8 MB and then washed to remove unbound plasmid. As controls, cells were also treated with neutral MBs plus 8 μg/mL plasmid free in solution, or no ultrasound treatment. (b) Comparison of sonoporation and Lipofectamine transfection methods on various adherent cell types. Cells were treated with 3.2 μg/mL plasmid and 4×10^7 MB/mL cationic or neutral MBs, or 0.13 μg/mL plasmid and Lipofectamine. Data shown as mean ± standard deviation for OptiCells (n = 4).

Table 1

Beam widths as a function of power intensity with a fixed 25% duty cycle

Power intensity (W/cm^2)	Acoustic negative pressure (MPa)	−6 dB Beam width (mm)
0.3	0.13	14.4
0.5	0.15	14.4
1.0	0.22	12.0
1.5	0.25	12.0
2.0	0.30	12.0
3.0	0.37	12.0
4.0	0.46	12.0
5.0	0.48	12.0

The transducer was positioned 50 mm away from the hydrophone in a 37 °C water bath. Acoustic pressure measurements, in 0.5mm size steps, were done along the transducer width, covering a total distance of 19 mm.

Table 2

Fluorescent markers used for the detection of phospholipid phosphatidylserine (PS) and nuclear/plasmid DNA binding

Name	Property	Detection method	Application
Annexin V	Membrane phospholipid PS marker	FACS	Identification of early apoptotic cells
GFP	Expression protein	FACS	GFP protein expression
YOYO-1	Fluorescent marker for DNA binding	FACS; Epifluorescence	Plasmid DNA conjugation to MBs
TOTO-3	Fluorescent marker for DNA binding	FACS	Intracellular delivery of plasmid DNA
7-AAD	Fluorescent marker for DNA binding	FACS	Identification of late apoptotic or necrotic cells

Flow cytometry (FACS) assessed measurements of GFP expression.